XI. GASEOUS ELECTRONICS*

Academic and Research Staff

Prof. G. Bekefi
Prof. S. C. Brown
Prof. J. C. Ingraham
Prof. B. L. Wright
Dr. W. M. Manheimer
J. J. McCarthy
W. J. Mulligan

Graduate Students

W. B. Davis
G. A. Garosi

A. CONTINUUM PROBE STUDIES OF A POSITIVE COLUMN IN FLOWING ARGON GAS

This report presents additional experimental results obtained on the apparatus reported upon previously.[1]

This apparatus produced a weakly ionized plasma (the positive column of a glow discharge) in a region of neutral-gas pipe turbulence. A movable probe assembly, described by R. L. Kronquist,[2] was added to permit data to be taken as a function of radius. The probe assembly was demountable to permit the probe to be changed quickly and conveniently. Furthermore, the tube diameter was increased to 2.2 cm in order to obtain the maximum flow permitted by the pumping capacity while maintaining the pressure in the discharge region at approximately 20 Torr.

It has been stated previously[1] that the electron temperature changed negligibly with increasing flow when compared with changes in the gas temperature. Electron temperature measurements for this tube were made with a double probe. The results substantiated the previous claim[1] and also showed that the electron temperature was essentially independent of radius (see Fig. XI-1).

The experimental data reported here were obtained from one or two electrostatic probes immersed in the plasma. Since the plasma is in a flowing medium, the time dependence of the probe signals will, in general, result from both an explicit time variation of the plasma parameters and from the passage of spatial variations past the probe. Under certain conditions, the explicit time variation can be neglected with the result that the spatial variations can be related to a frequency through

$$f = \frac{\overline{U}}{\ell}, \qquad (1)$$

where $\overline{U}$ is the mean flow velocity, and ℓ is the length, in the axial direction, of the spatial inhomogeneity. In the absence of shear flow the condition for Eq. 1 to hold is given[3] by

*This work was supported by the Joint Services Electronics Programs (U.S. Army, U.S. Navy, and U.S. Air Force) under Contract DA 28-043-AMC-02536(E).

$$5\frac{U_1'^2}{\overline{U}^2} \ll 1, \tag{2}$$

where U_1' is the rms value of the axial component of the fluctuating velocity. Since the criteria for the validity of Eq. 1 in the presence of shear flow is unknown, it must be checked experimentally.

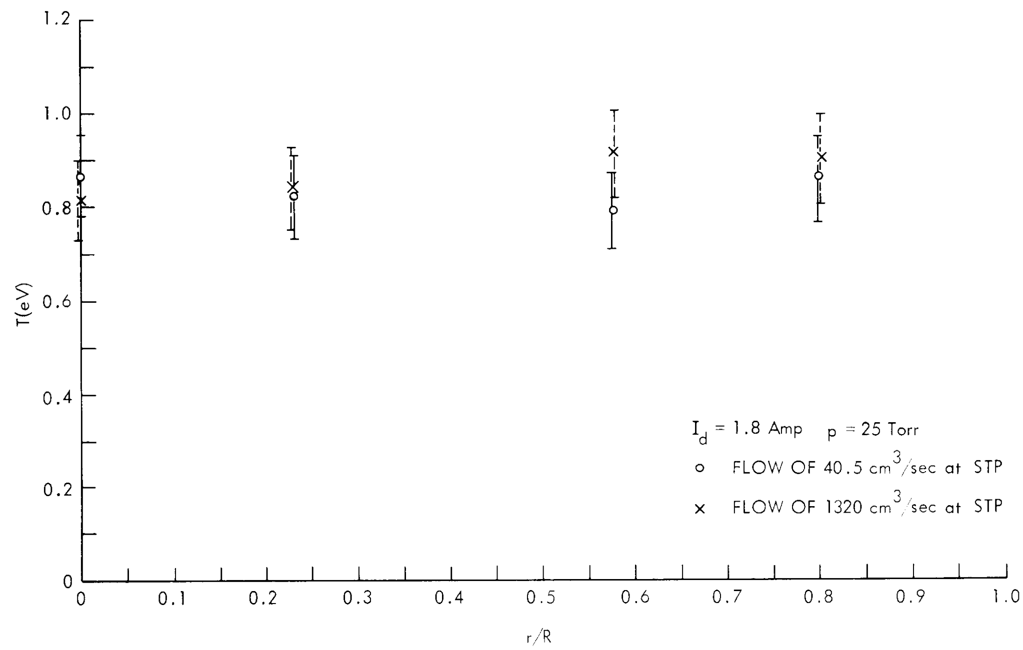

Fig. XI-1. Electron temperature from double-probe curves.

One method, described by V. L. Granatstein,[4] is to compare the plasma density spectrum for different flow velocities while keeping the Reynolds number, Re, constant. If the frequency scale of the spectrum analyzer is varied so that $f/\overline{U}$ remains unchanged, then, according to Eq. 1, the resulting spectra should be similar. Another method involves the use of the frequency spectra of the fluctuating floating potential and electric field in the plasma. The electric field was measured by taking the output of two floating probes oriented in the axial direction and separated by 0.5 mm and feeding them into a Tektronix 1A6 differential preamplifier. This procedure was superior to that described previously.[1]

The spectrum of the potential is related to that of the electric field by

$$F_E(k_1) \propto k_1^2 F_\phi(k_1), \tag{3}$$

where k_1 is the axial wave number of the eddy, and $F_E(k_1)$ and $F_\phi(k_1)$ are the electric field and potential spectra, respectively. In terms of wave number Eq. 1 becomes

$$k_1 = \frac{2\pi f}{\overline{U}}. \tag{4}$$

Combining Eqs. 3 and 4 yields

$$20 \log_{10}\left(\frac{f}{f_o}\right) = 10 \log_{10} \frac{F_E(f)}{F_E(f_o)} - 10 \log_{10} \frac{F_\phi(f)}{F_\phi(f_o)}, \tag{5}$$

where f_o is a convenient normalizing frequency necessary to remove the unknown proportionality constant in Eq. 3. If it is assumed that instead of Eq. 4 the following relationship holds

$$k = \frac{2\pi f^a}{U^b}, \tag{6}$$

where a and b are any real numbers, then Eq. 5 may be replaced by

$$20a \log_{10}\left(\frac{f}{f_o}\right) = 10 \log_{10} \frac{F_E(f)}{F_E(f_o)} - 10 \log_{10} \frac{F_\phi(f)}{F_\phi(f_o)}. \tag{7}$$

Thus a plot of the right-hand side of Eq. 7 against log f should yield a straight line with a slope of 20 if Eq. 4 is valid. The results of this analysis are shown in Fig. XI-2. Thus, to a good approximation, the use of Eq. 1 is justified for Reynolds numbers

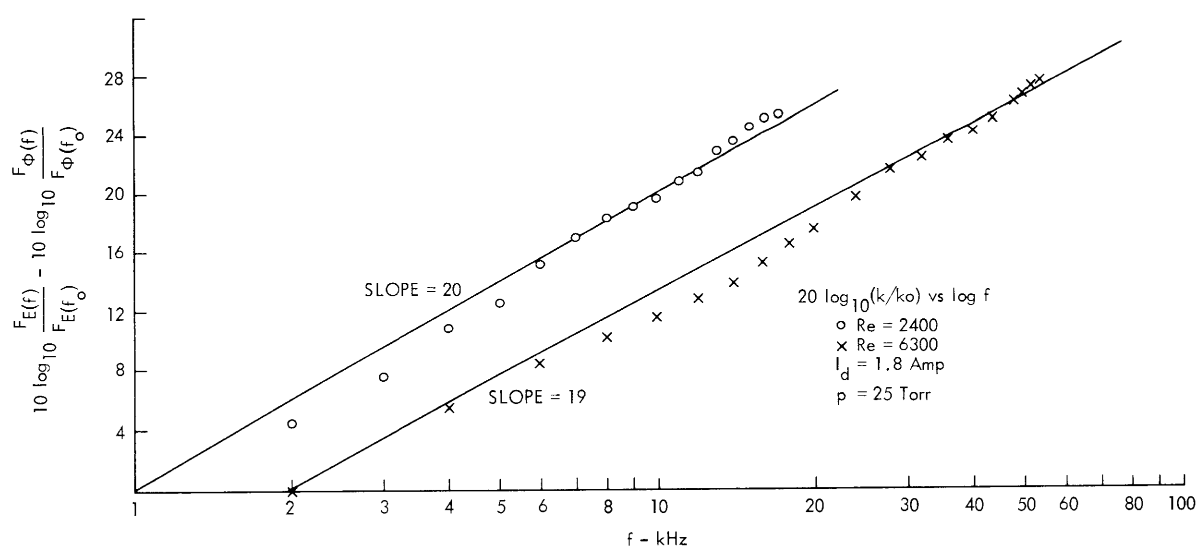

Fig. XI-2. Check of frozen-flow assumption (Eq. 4).

between 2400 and 6000 and the resulting flow is referred to as frozen flow.

The behavior of the plasma density and axial electric field with flow was very similar to that reported previously.[1,4] The floating potential was also measured, and its behavior was similar to that of the plasma density and electric field. An explanation of the potential (or electric field) behavior is still being sought.

The development with flow of plasma density inhomogeneities of various sizes can be observed by using a bandpass filter as previously shown.[1] The bandpass filter that was

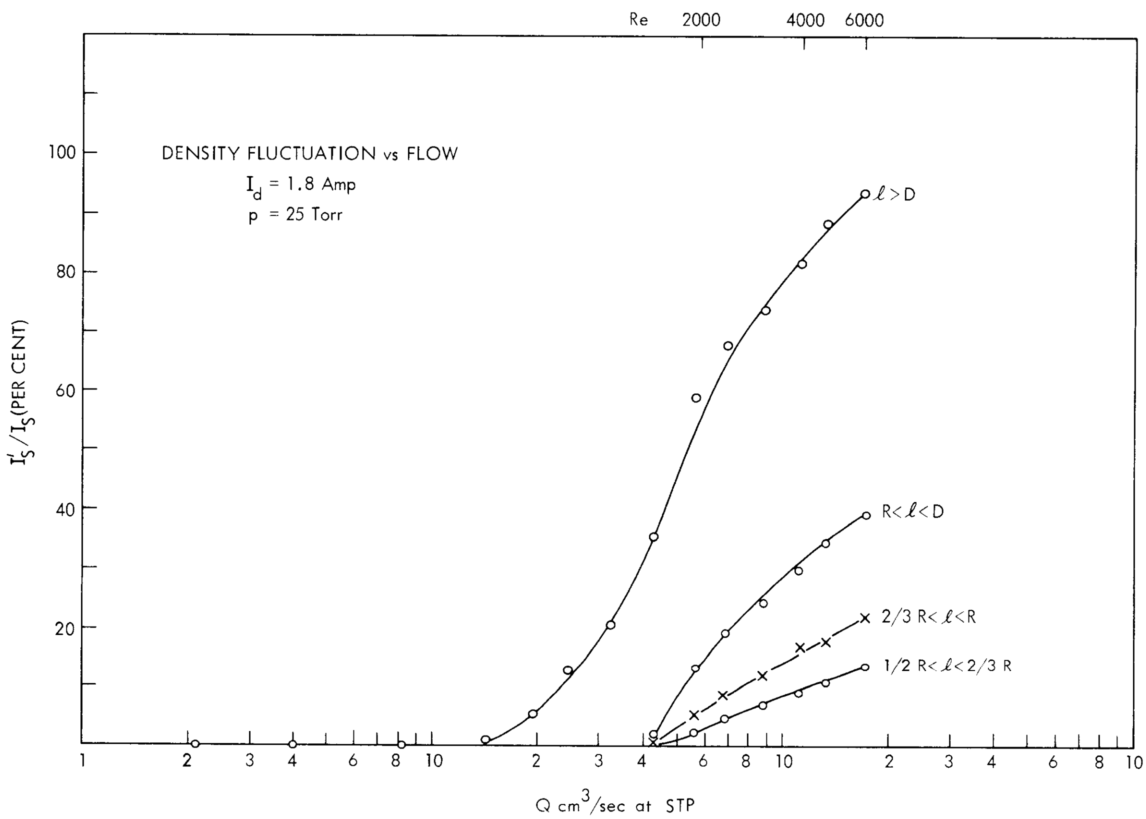

Fig. XI-3. Development of plasma density eddies.

used was a Spencer-Kennedy Laboratory Model 302 which has an 18 dB/octave frequency rolloff. The data, plotted in Fig. XI-3, shows that, although the large-scale fluctuations begin at very low flows, the inhomogeneities with axial scale lengths ℓ, such that $\ell \ll D$, do not appear until the flow attains a Reynolds number of ~1500, where D is the tube diameter. The results also show that the larger eddies grow in intensity more rapidly than the smaller eddies do and that they all show a tendency to saturate. (Note that the abscissa scale is logarithmic.)

Measurements made by Granatstein[4] showed that the intensity of the large-scale plasma density fluctuations, $\ell \gtrsim D$, had a radial profile similar to that of the mean plasma density gradient. This effect was observed in this experiment for medium flows, but for the larger flows it was not seen (see Fig. XI-4). This discrepancy is being

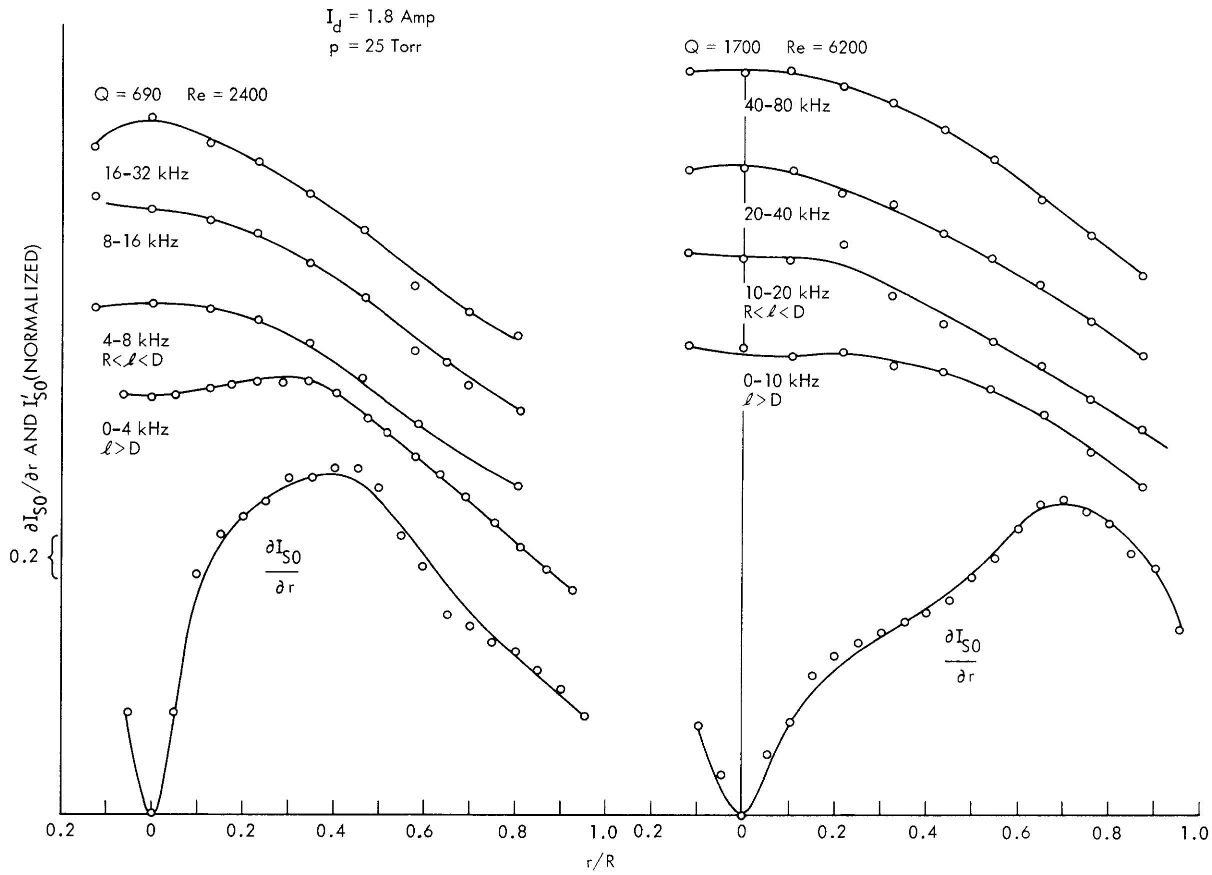

Fig. XI-4. Density fluctuation and density gradient profiles.

investigated. There are some indications that the answer may be in the behavior of the very large inhomogeneities.

The tendency of turbulence to smooth out gradients in any of the properties of the medium is shown by the effect of increased flow on the mean plasma density profile (see Fig. XI-5). The zero-order Bessel function is plotted for reference; this is the predicted profile for a diffusion-dominated discharge. Argon shows a bell-shaped profile for the low flows as a result of the rapid increase with energy of the electron-neutral scattering cross section.[5] Note that for the larger flows the density profile becomes flatter than that associated with a diffusion-dominated discharge. The initial contraction in going from a flow of 82.5 cm^3/sec at STP to 242 cm^3/sec is still unexplained.

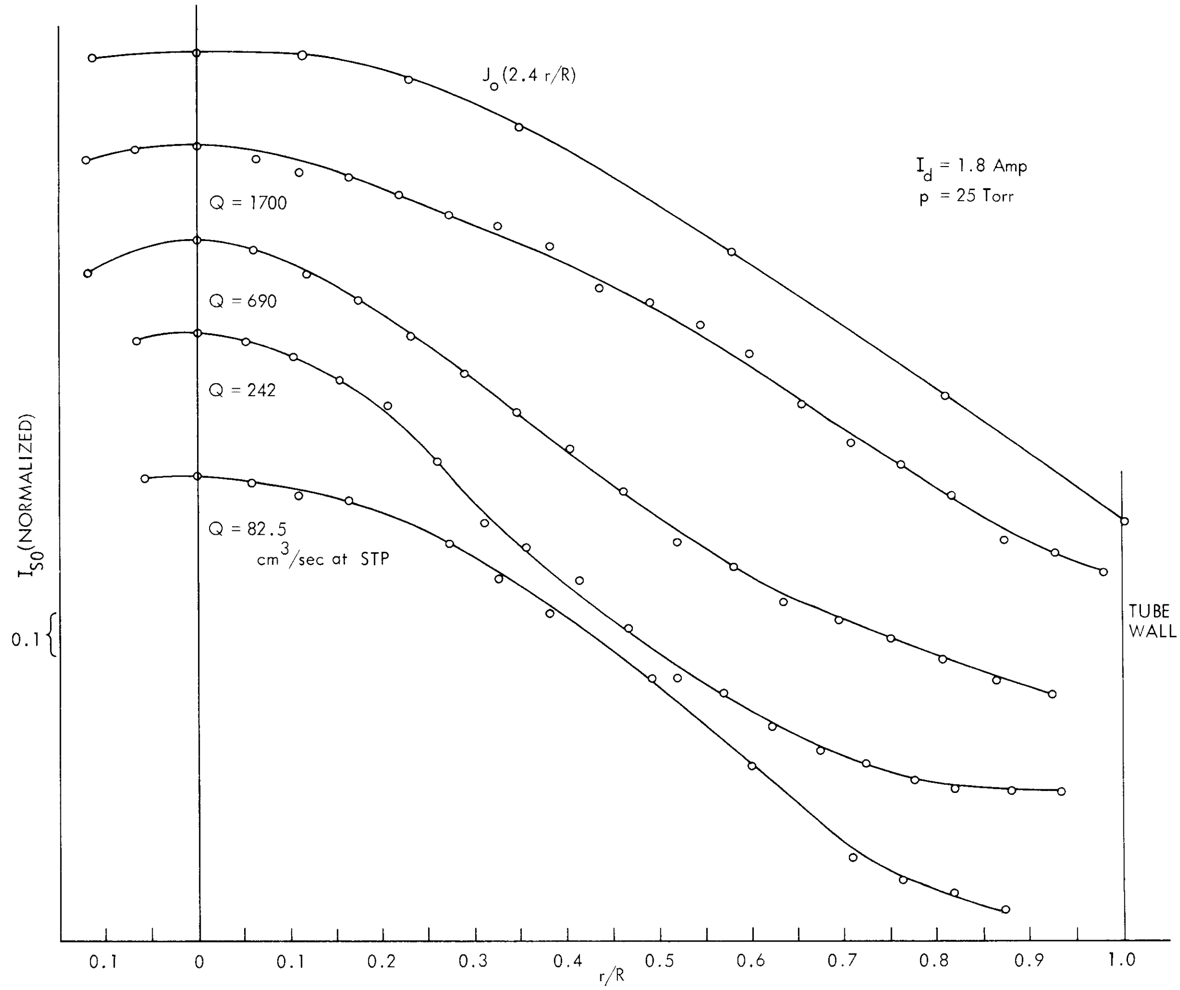

Fig. XI-5. Density profile normalized to unity on axis.

Radial profiles for the floating potential and for the axial electric field are plotted in Fig. XI-6. Comparing this with Fig. XI-5, we see that there is a strong similarity between the potential, axial electric field and the plasma density. Further analysis is necessary to explain fully the origin of the potential fluctuations.

As stated above, it is the floating potential, ϕ_f, which is measured; however, it is the plasma potential, ϕ_p, which is related to the electric field in the plasma by

$$E = -\nabla\phi_p, \tag{8}$$

where the vector potential has been neglected, because of the very low frequencies involved. It is thus necessary to compute the error involved in using the floating potential.

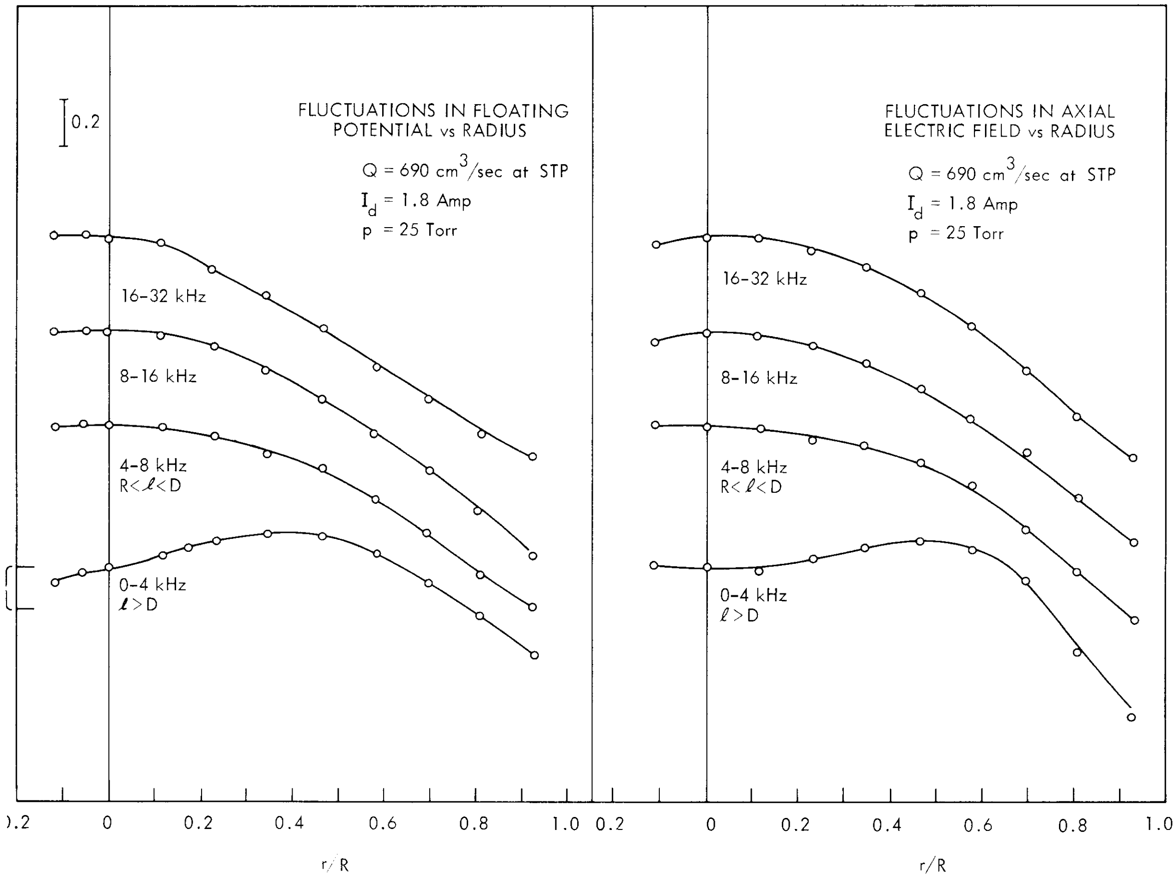

Fig. XI-6. Radial profiles for the floating potential and the axial electric field.

It can readily be shown by using the expression

$$\phi_p = \phi_f + V_o \tag{9}$$

that the fluctuating components of the potential satisfy

$$\overline{(\phi_p')^2} = \overline{(\phi_f')^2} + \overline{(V_o')^2} + 2\,\overline{\phi_f' V_o'}, \tag{10}$$

where the bar represents time average, and the prime denotes the fluctuating component so that

$$\begin{aligned} \phi_p &= \overline{\phi_p} + \phi_p' \\ \phi_f &= \overline{\phi_f} + \phi_f' \qquad \overline{\phi_p'} = \overline{\phi_f'} = \overline{V_o'} = 0 \\ V_o &= \overline{V_o} + V_o' \end{aligned} \tag{11}$$

An expression for the potential difference, V_o, between a cylindrical probe at floating potential and the plasma has been given by Zakharova et al.[6]

$$e^{V_o/T_-} = .02\sqrt{\frac{T_-}{AT}}\,\frac{\lambda_+}{r_p}\,\frac{1}{\ell n\left[\frac{\ell_p}{r_p(1+u)}\right]}\,\frac{1-\frac{9}{20}\frac{ur_p}{\lambda_-}\frac{T_-}{V_o}}{1+.015\frac{\lambda_+}{\lambda_-}\frac{T_-}{V_c}\sqrt{\frac{T_-}{AT}}}, \tag{12}$$

where T_- and T are the electron and ion temperatures in electron volts, respectively, ℓ_p is the probe length, r_p is the probe radius, ur_p is the sheath thickness, λ_+ and λ_- are the ion and electron mean-free paths, respectively, A is the atomic weight of the ions, and V_c is the potential difference between the undisturbed plasma and the sheath edge. Note that both V_o and V_c are negative for a floating probe.

For the parameters of this experiment Eq. 12 reduces to

$$e^{V_o/T_-} = \frac{B}{\alpha - \ell n(1+u)}, \tag{13}$$

where $\alpha = \ell n\left(\frac{\ell_p}{r_p}\right) = 1.9$, and $B = 0.02\sqrt{\frac{T_-}{AT}}\,\frac{\lambda_+}{r_p}$.

In order to obtain V_o, it was assumed that fluctuations in the sheath thickness were proportional to fluctuations in the Debye length, λ_D, where

$$\lambda_D = \sqrt{\frac{\epsilon_o T_-}{ne}}, \tag{14}$$

and n is the plasma density. Although this assumption is reasonable, it has not yet been possible to verify that it is consistent with the expression for u given by Zakharova et al.[6]

$$u = 0.23\,\frac{1}{r_p}\left[\frac{|v_o|^3\lambda_+}{J_+^2 A}\right]^{1/5}, \tag{15}$$

where J_+ is the ionic current density in ma/cm^2. It is also assumed, for reasons given by Granatstein,[4] that fluctuations in T_- can be neglected.

By using the assumption above and Eqs. 13 and 14, and dividing by $\overline{(\phi_f')^2}$, Eq. 9 becomes

$$\frac{\overline{(\phi_p')^2}}{\overline{(\phi_f')^2}} = 1 + \left[\frac{T_-}{2[a-\ln(1+u)]\left[1+\frac{1}{u}\right]}\right]^2 \frac{\overline{(n')^2}}{\overline{n}^2} \frac{1}{\overline{(\phi_f')^2}}$$

$$+ 2\rho(\phi_f', V_o') \left[\frac{T_-}{2\left(1+\frac{1}{u}\right)[a-\ln(1+u)]}\right] \frac{\sqrt{\overline{(n')^2}}}{\overline{n}} \frac{1}{\sqrt{\overline{(\phi_f')^2}}}, \tag{16}$$

where

$$\rho(\phi_f', V_o') = \frac{\overline{\phi_f' V_o'}}{\sqrt{\overline{(\phi_f')^2}}\sqrt{\overline{(V_o')^2}}}$$

is the correlation coefficient. To evaluate Eq. 16, ρ is set equal to one, since this gives the worst case. For the worst condition present in this experiment we obtain

$$\left[\frac{\overline{(\phi_p')^2}}{\overline{(\phi_f')^2}}\right]^{1/2} \approx 1.14.$$

Thus using the floating potential results in an error of approximately 14% at worst and is generally much better.

It is possible to obtain the scale size of the smallest eddies by means of the two-point correlation. For homogeneous turbulence the two-point plasma density correlation coefficient reduces, for sufficiently small separation,[7] to

$$R_{\gamma,\gamma}(r) = 1 - \frac{r^2}{\lambda_\gamma^2}, \tag{17}$$

where λ_γ is the microscale for the density fluctuations, and r is the separation of the two observation points. For the condition of frozen flow it is possible to obtain the axial scale length for density fluctuations by means of the temporal correlation at one point (autocorrelation). Then the autocorrelation, for sufficiently short delay time, is given[8] by

$$R_{E,\gamma}(t) = 1 - \frac{t^2}{\tau_{E,\gamma}^2}, \tag{18}$$

where $\tau_{E,\gamma} = \lambda_\gamma/\overline{U}$.

The autocorrelation was taken with a Honeywell 9410 correlation, and the expected parabolic section was observed. A plot of $1 - R_E(t)$ against t^2 yielded a straight line

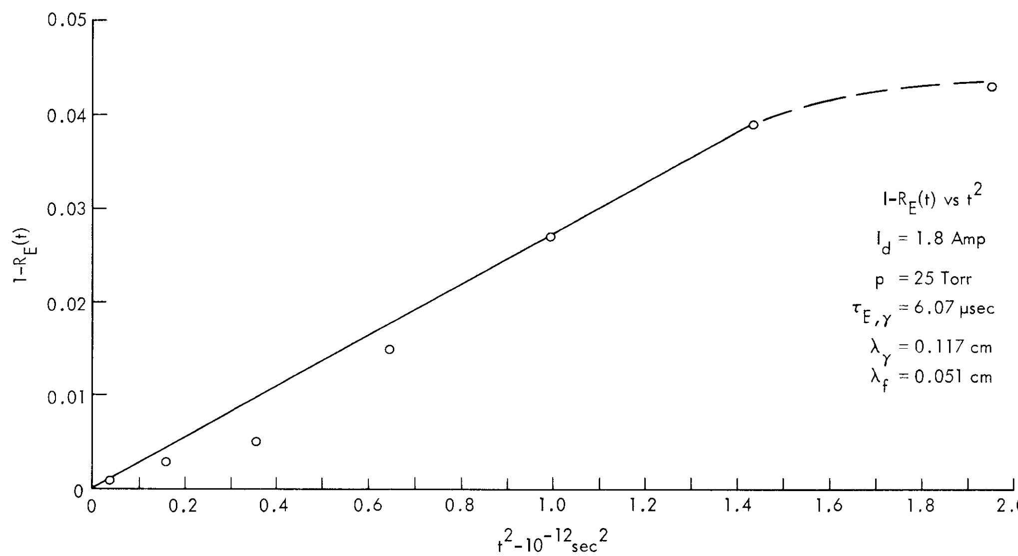

Fig. XI-7. Microscale length.

over the first two microseconds and gives a value of $\tau_{E,\gamma}$ of 6.07 μsec (see Fig. XI-7) or a microscale length of 0.117 cm. This scale length for the plasma density fluctuations can be related to longitudinal neutral-gas velocity scale length by

$$\frac{\lambda_\gamma}{\lambda_f} = \sqrt{\frac{D}{\nu}}, \tag{19}$$

where λ_f is the microscale length for velocity fluctuations in the axial direction, D is the diffusion coefficient for the plasma, and ν is the kinematic viscosity. For the parameters of the discharge used in getting Fig. XI-7, Eq. 19 yields $\lambda_\gamma/\lambda_f \approx 2.3$.

Thus the smallest inhomogeneities in the plasma density are approximately one-tenth the tube radius, and approximately twice as large as the smallest eddies in the neutral gas.

Future work includes a complete analysis in order to explain many still unexplained effects, the addition of a grid at the input to the discharge pipe, and an attempt to measure directly the expected but unconfirmed enhanced plasma loss rate caused by the turbulence. The grid is being added, since it is possible that it will have an effect on the very low frequency (large-scale length) fluctuations.

G. A. Garosi

References

1. G. A. Garosi, "Effects of Hydrodynamic Turbulence on a Weakly Ionized Argon Plasma," Quarterly Progress Report No. 86, Research Laboratory of Electronics, M.I.T., July 15, 1967, pp. 129-134.

2. R. L. Kronquist, "Microwave Scattering from an Electron-Beam Produced Plasma," Quarterly Progress Report No. 82, Research Laboratory of Electronics, M.I.T., July 15, 1966, pp. 109-114.

3. J. O. Hinze, Turbulence (McGraw-Hill Book Company, Inc., New York, 1959), p. 41.

4. V. L. Granatstein, "Structure of Wind-Driven Plasma Turbulence as Resolved by Continuum Ion Probes," Phys. Fluids 10, 1236 (1967).

5. H. M. Schulz III, "Interactions of Electrons and Acoustic Waves in a Plasma," Ph.D. Thesis, M.I.T., 1967.

6. V. M. Zakharova et al., Soviet Phys. – Tech. Phys. 5, 411 (1960).

7. J. O. Hinze, ibid., p. 220.